Observed Foreshock Ions which are Actually Behind the Martian Bow Shock

R. A. Frahm[(1)], M. Yamauchi[(2)], J. D. Winningham[(1)], R. Lundin[(2)], J. R. Sharber[(1)], H. Nilsson[(2)], A. J. Coates[(3)], and J. Mukherjee[(1)]

[(1)] Southwest Research Institute, 6220 Culebra Road, San Antonio, TX 78228, USA [(2)] Swedish Institute of Space Physics, Box 98128 Kiruna, Sweden [(3)] Mullard Space Science Laboratory, University College London, Dorking RH5 6NT, UK

Abstract

The Mars Express (MEx) analyzer of space Plasmas and Energetic Atoms (ASPERA-3) experiment contains ion and electron instruments for conducting plasma measurements. On January 23, 2012, during in-bound travel of MEx in the southern hemisphere of Mars traveling from its dawn side toward periapsis at dusk, the plasma instruments measured foreshock-like ion beams extending from outside the bow shock and into the magnetosphere, continuing to a distance of about a proton gyroradius from the bow shock. These ion beams were mostly protons, were observed to have energies greater than solar wind protons, and were not gyrating, in agreement with reflections of the solar wind proton beam. Furthermore, in the foreshock region, the ion energy gradually decreased toward the magnetosheath, in agreement with an acceleration by an outward-directed electric field in the bow shock. The observations also suggest that this electric field exists even inside the magnetosheath, within the distance of a proton gyroradius from the bow shock.

Introduction

Although Mars possesses a small intrinsic magnetic field, the interaction is with an ionized, conducting, spherical ionosphere, formed largely by photoionization of the upper atmosphere. In this ionosphere currents flow so as to exclude the solar wind and magnetic field from altitudes below a few hundred kilometers at the subsolar point. Due to the supersonic speed of the solar wind, a bow shock is formed upstream of the planet and the oncoming solar wind is shocked, then diverted in the magnetosheath around the planet [Luhmann, 1995].

Part of the solar wind interaction that creates the bow shock can generate a foreshock region of reflected and accelerated electrons and ions. The foreshock is dependent on the interplanetary magnetic field (IMF) and its connection to the bow shock. When the angle between the IMF and bow shock normal is greater than 45°, the shock is quasi-perpendicular and the foreshock region is restricted to near the shock foot [Bale et al., 2005]. For an angle less than 45°, the shock is termed quasi-parallel [Burgess et al., 2005] and the foreshock has a much larger domain. For quasi-parallel shocks, the electron foreshock is observed antisunward of the sunward-most IMF field line which connects to the bow shock [Eastwood *et al.*, 2005; Yamauchi *et al.*, 2011] with the ion foreshock more tailward than this location (see examples, Burgess, 1995; Parks, 2004; Eastwood *et al.*, 2005)

Instrumentation

Plasma is measured on the Mars Express (MEx) spacecraft by the Analyzer of Space Plasmas and Energetic Atoms (ASPERA-3) experiment [Barabash et al., 2004; 2006]. Ions are measured with the Ion Mass Spectrometer (IMA), which has a top hat energy deflection system coupled with an entrance elevation analyzer and an exit magnetic momentum analyzer. For this study, 50 eV to 20 keV ions are measured logarithmically in 66 energy steps and linearly below 50 eV in 30 steps (96 total energy steps). IMA measures from 360° of azimuth with 16 angular sectors, each 22.5° wide. In elevation, IMA measures from -45° to +45° above 50 eV energy in 16 elevation sectors, each about 5.6° wide. Below 50 eV, elevation scanning is disabled and the ions are measured from 0° elevation, about 5.6° wide. The momentum analyzer separates ions into a 32 mass channel array. Ions up to 40 amu are collected, simultaneously. The entire energy-angle-mass array is accumulated in 192 s. Each energy-azimuthal angle scan at a single elevation angle occurs in 12 s. Electrons are measured by the Electron Spectrometer (ELS). ELS is a spherical top hat analyzer which is mounted on a scanner. For these data, the scanner angle was fixed so that the ELS and IMA central plane are roughly perpendicular. The ELS measures from 360° with 16 azimuth bins, each 22.5° wide. The angular width is ±2°. ELS measured a 127 step energy spectrum from 0.5 eV to 20 keV logarithmically in 4 s.

Orientation

The spacecraft entered the Mars system on the dawn side in the southern hemisphere and preceded to periapsis on the dusk side about 2343 UT. **Figure 1** aids in visualizing the MEx trajectory. Shown are views in the Mars Solar Orbital (MSO) coordinate system: MSO X-Y, X-Z, and Y-Z planes as well as in cylindrical coordinates. The average locations of the bow shock and the Magnetic Pileup Boundary (MPB) [Vignes *et al.*, 2000] are indicated on **Figure 1d**. The average position of the bow shock occurs at about 2222 UT and the average position of the MPB occurs at about 2307 UT. In general, the MPB is defined using a magnetometer; and since MEx contains no magnetic field experiment, MEx measures the Induced Magnetospheric Boundary (IMB) [Lundin *et al.*, 2004] from the particle signatures. However, the MPB and IMB are very nearly co-located.

The solar wind ions are closely aligned with the Sun direction. For the time at which the data were taken, between measurement of the solar wind at 2145 UT until measurement in the magnetosheath at 2240 UT, the Sun vector at MEx was between 78° and 84° with respect to the spacecraft spherical polar angle, θ. With the 22.5° azimuth sectors of IMA, the boundary between IMA azimuth sector 0 and sector 1 occurs at a spacecraft θ of 67.5°, so the solar wind ion beam should be strongest in IMA azimuth sector 0 with some smaller portion in IMA azimuth sector 1. In spacecraft azimuthal angle, φ, the Sun is located at 180° for the region of the bow shock. This translates to an IMA elevation angle of 0° (the central measurement plane), between elevation sectors 7 and 8. A rough orientation shows that elevation scanning occurs parallel to the ecliptic plane and azimuth scanning occurs perpendicular to the ecliptic plane.

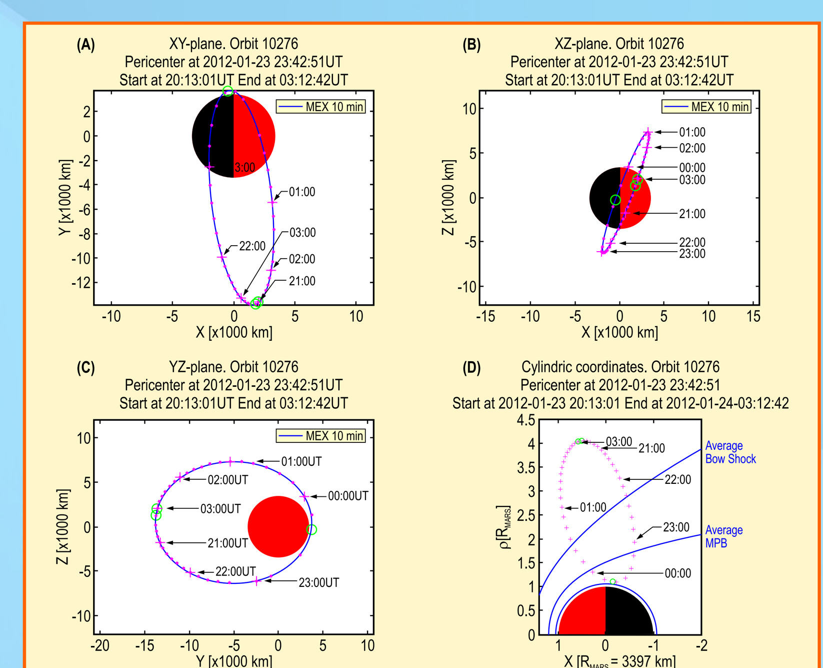

***Figure 1**. Mars Express Trajectory on 23 January 2012. Shown are the trajectory of the Mars Express spacecraft in the X-Y (a), X-Z (b), and Y-Z (c) planes in km for the MSO coordinates for the pass of the spacecraft shown in Figure 2. The Cartisian system is combined into a cylinderical representation and shown in terms of the Mars radius of 3397 km (d) with the central axis along the MSO X direction shown in the horizontal direction and the amplitude of the radial vector shown in the vertical direction. Two blue curves represent the average locations of the bow shock and Magnetospheric Pileup Boundary (MPB) [Vignes et al., 2000]. In all panels, the location of the pericenter time is marked by a single green circle near the planet and the location of the apocenter time is marked with dual green circles indicating the beginning/ending definition of a MEx orbit.*

Observations

An overall picture of the pass is shown in **Figure 2**. Measurements begin in the solar wind at 2145 UT on January 23, 2012 and the MEx spacecraft progressed inbound from the solar wind in the southern hemisphere around dawn, reaching perigee on the dusk side of Mars near the equator in the northern hemisphere at about 350 km altitude. Shown in the top panel is the background corrected electron spectra from sector 4, and the center panel shows the ion spectrogram from sector 0. In both cases, the color range is adjusted to highlight specific features within the spectrograms. The ion flux values less than 5.0×10^{-7} ergs/(cm^2 s sr eV) have been removed. The spacecraft position information is shown in the bottom panel.

At the beginning of the pass, the ion spectral data indicated a steady solar wind at about 380 km/s. The dot pattern occurs because the elevation analyzer measures ions as a function of time over a range of elevations and only encounters the solar wind proton beam at elevations near the central axis of the instrument. At about 2207 UT, foreshock-like ions were observed as a peak in the ion spectrum at higher energy than the solar wind H^+ and He^{++}, and at a different elevation angle with respect to the solar wind beam.

Background adjusted electron measurements indicate that the electron foreshock was detected beginning between 2157 UT to 2202 UT when the spacecraft was about 8000 km away from the surface of Mars. During this time, the solar wind electrons were observed to be stable and the core showed a slight increase in intensity from that in the solar wind; the halo/strahl electrons of the solar wind are observed to increase slightly.

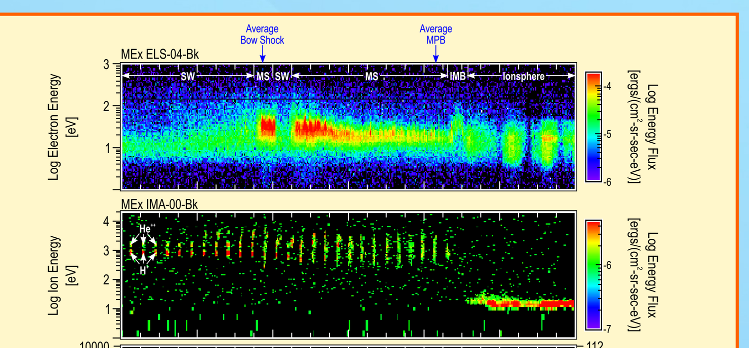

2012/023	21:45	22:05	22:25	22:45	23:05	23:25	23:45
MSO X [km]	-566.35	-1074.26	-1528.74	-1873.54	-1992.78	-1614.48	-295.36
MSO Y [km]	-1.1e+04	-9441.78	-7372.51	-4799.13	-1692.76	1714.53	3743.51
MSO Z [km]	-4387.95	-5345.55	-6043.46	-6315.65	-5840.81	-3941.33	155.84
Pd LAT [deg]	152.25	147.38	142.51	137.63	132.76	127.89	123.01
SolTime [hr]	-32.95	-41.33	-51.64	-65.37	-85.18	-56.40	12.48
	5.80	5.57	5.22	4.58	2.69	20.89	18.30

***Figure 2**. Inbound Charged Particle Measurements from the Solar Wind to Periapsis. The top panel shows an energy-time spectrogram in differential energy flux of the ASPERA-3 electrons from ELS sector 04 with the plasma regions marked (SW = solar wind, MS = magnetosheath). The center panel shows an energy-time spectrogram in differential energy flux (DEF) of the ASPERA-3 ions from IMA sector 00 with the first three locations on solar wind ions noted. The bottom panel shows the spacecraft altitude and solar zenith angle with the MSO position, Planetodetic longitude and latitude, and solar time. The average positions of the bow shock and MPS shown in Figure 1d are indicated at the top. Both electron and ion spectra have background removed. Ion energy flux values below 5.0×10^{-7} ergs/(cm^2 s sr eV) are excluded.*

Discussion

The region of interest is from the ion foreshock beginning at about 2205 UT and lasting until the ions penetrate the last bow shock at about 2240 UT. **Figure 3** numbers the ion cycles in the ion spectrogram. Circles indicate observations of foreshock and foreshock-like ions. Foreshock ions are observed in the foreshock region. Foreshock-like ions have similar distribution and composition as discrete type foreshock ions [Yamauchi *et al.*, 2011, 2015], but are observed beyond the foreshock region. Foreshock and foreshock-like ions are observed both flowing at an angle offset to that of the solar wind and at multiples of H^+ energy in the solar wind. Unfortunately since MEx carries no magnetometer, we cannot determine the deHoffmann-Teller frame of the bow shock.

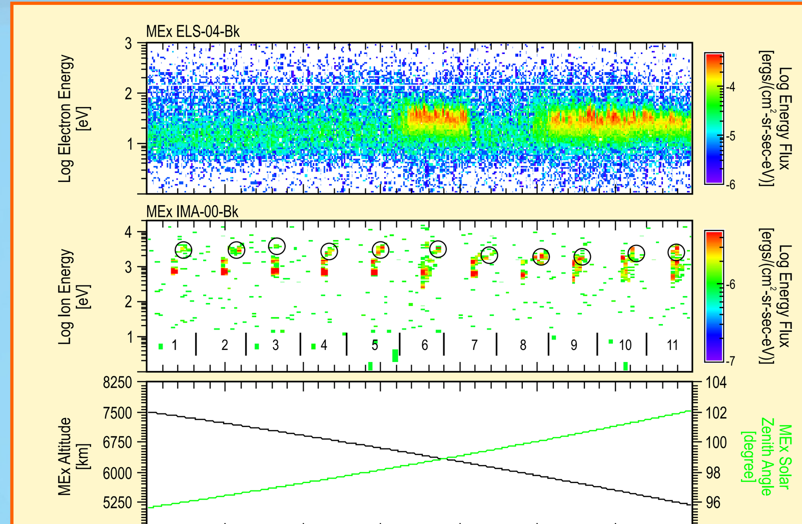

2012/023	22:05	22:10	22:15	22:20	22:25	22:30	22:35	22:40
MSO X [km]	-1074.26	-1194.60	-1310.72	-1422.51	-1528.74	-1628.38	-1719.90	-1802.32
MSO Y [km]	-9441.78	-8968.34	-8467.38	-7935.28	-7372.51	-6778.09	-6152.98	-5492.94
MSO Z [km]	-5345.55	-5549.42	-5734.85	-5900.60	-6043.46	-6160.38	-6247.50	-6301.05
Pd LON [deg]	147.38	146.16	144.94	143.73	142.51	141.29	140.07	138.85
Pd LAT [deg]	-41.33	-43.68	-46.17	-48.82	-51.64	-54.67	-57.94	-61.49
SolTime [hr]	5.57	5.49	5.41	5.32	5.22	5.10	4.96	4.79

***Figure 3.** Foreshock, Bow Shock, and the Outer Magnetosheath of Mars on 23 January 2012. The format is similar to Figure 2, but the color range and time scale are adjusted to reveal more detail. The ion cycles of a complete energy-elevation scan are marked. The solar wind hydrogen is indicated as the red spot at the lowest energy for each measurement cycle. Foreshock-like ions are circled.*

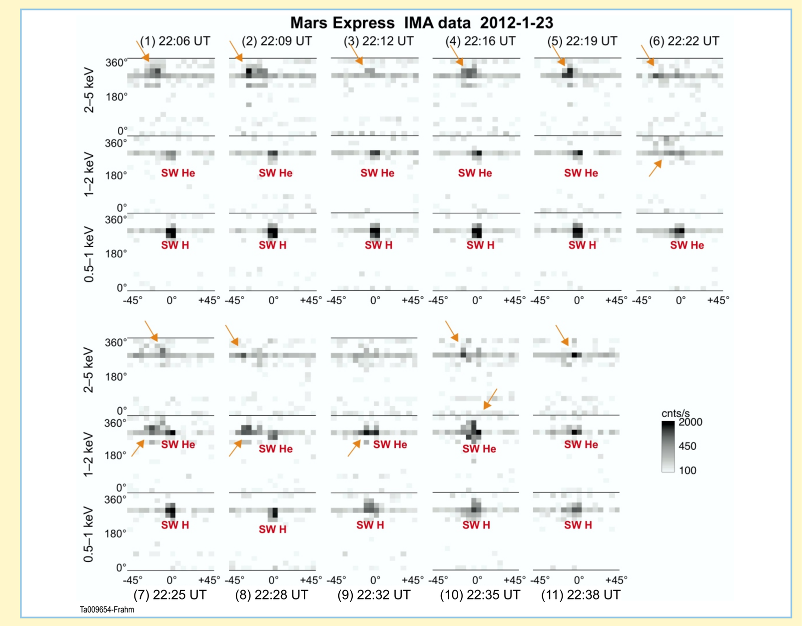

***Figure 4.** Instrument Angular View. Shown are 11 angular view spectrograms corresponding to the cycles marked in Figure 4. Each is marked with the approximate center time of the measurement cycle and the cycle number. Along each vertical axis is the instrument azimuth rotated by 180° to display the solar wind in the center (0° to 360°) and each horizontal axis is the instrument elevation (-45° to +45°). Angular spectrograms for three integral energy bands (0.5-1 keV, 1-2 keV, and 2-5 keV) are shown in a stacked configuration. Locations of the solar wind (SW) hydrogen (H) and helium (He) are indicated. Arrows point to foreshock/foreshock-like ions.*

Figure 3 shows electron measurements that indicate three shock transitions at about 2221 UT, 2225:30 UT, and 2230 UT. Shocked plasma suggests that the spacecraft encountered conditions which caused an earlier bow shock at 2221 UT to be detected with penetration into the magnetosheath followed by a reverse shock (shocked plasma to unshocked plasma) at 2225:30 UT with solar wind plasma again observed. The bow shock transition observed at about 2330 UT indicates the spacecraft's passing into the magnetosheath. These transitions are also indicated by the ions, as the solar wind H+ indicates more heating at elevations around the solar wind H^+ beam when the solar wind penetrates into the magnetosheath [Lundin *et al.*, 2006].

The angular deviations of ions are shown in **Figure 4** by examining three important energy ranges: 0.5-1 keV, 1-2 keV, and 2-5 keV. In these angular presentations, each vertical axis shows the instrument azimuth rotated by 180°, so that the solar wind appears in the plot center (0° to 360°) and each horizontal axis shows the instrument elevation (-45° to +45°). The approximate center time of the measurement cycle and the cycle number is indicated. The integral energy band 0.5-1 keV shows the angular location of the solar wind H^+ while the integral energy band 1-2 keV indicates mainly the solar wind He^{++}, but also shows some foreshock-like ions which are separated in angular space from the solar wind direction (indicated by arrows in **Figure 4**). The 2-5 keV integral energy band shows foreshock and foreshock-like ions, separated from the solar wind both in energy and angle. Angular differences between foreshock ions and the solar wind direction are on average 30°-40°. This means that the foreshock/foreshock-like ions are flowing toward the tail of Mars.

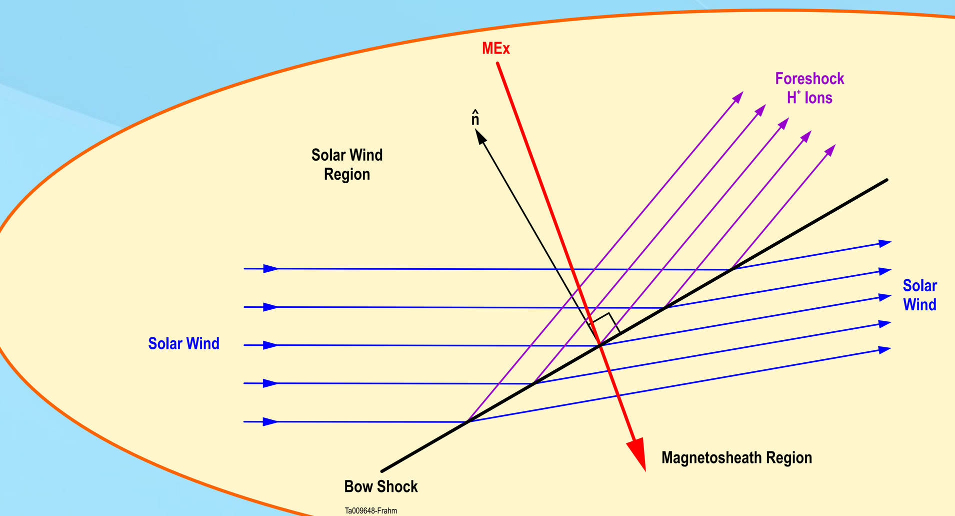

***Figure 5.** Creation of foreshock ions at the bow shock. The solar wind (blue) intersects the bow shock (black) creating a transmitted component (blue) of solar wind ions and a reflected component (purple) of foreshock ions (after Yamauchi et al., 2015). Reflected ions are accelerated by an electric field in the bow shock due to the magnetic field and solar wind velocity to cause the foreshock ions to have energies that are multiples of the solar wind energy.*

Conventional theory describing how foreshock ions are created is discussed in Yamauchi *et al*., [2015] and is illustrated in **Figure 5**. **Figure 5** represents a small portion of the bow shock where the solar wind ions (blue) are transmitted through and reflected off the bow shock, creating the fraction inside and flowing closer to the boundary to satisfy the shock jump conditions [Burgess, 1995; Parks, 2004] (blue). The fraction reflected becomes the foreshock population (purple). Parks [2004] and Yamauchi *et al*. [2006] describe how the electric field accelerates ions encountering the shock by a change in the cross product of the velocity of the particle and the magnetic field. The flow in the presence of the magnetic field generates an outward-directed electric field in the bowshock. Creation of foreshock ions at multiples of the flow energy are generated in agreement with the observed foreshock ions.

References

Bale, S. D., M. A. Balikhin, T. S. Horbury, et al., Quasi-perpendicular shock structure and processes, *Space Sci. Rev.* **118**, 161–203, DOI: 10.1007/s11214-005-3827-0, 2005.

Burgess, D., Collisonless Shocks, in Introduction to Space Physics (Cambridge University Press, Cambridge, UK) ed. M. G. Kivelson and C. T. Russell, 129-163, 1995.

Burgess, D., E. A. Lucek, M. Scholer, et al., Quasi-parallel shock structure and processes, *Space Sci. Rev.* **118**, 205–222, DOI: 10.1007/s11214-005-3832-3, 2005.

Barabash, S. R. Lundin, H. Andersson, et al., ASPERA-3: Analyser of Space Plasmas and Energetic Ions for Mars Express, in MARS EXPRESS: The Scientific Payload, ed. A. Wilson, European Space Agency Publications Division, European Space Research & Technology Centre, Noordwijk, The Netherlands, SP-1240, 121-139, 2004.

Barabash, S., R. Lundin, H. Andersson, *et al.*, The Analyzer of Space Plasmas and Energetic Atoms (ASPERA-3) for the Mars Express mission", *Space Sci. Rev.*, **26**, 113-164, 2006.

Eastwood, J. P., E. A. Lucek, C. Mazelle, et al., The foreshock, *Space Sci. Rev.*, **118**, 41-94, doi:10.1007/s11214-005-3824-3, 2005.

Luhmann, J. G., Plasma interactions with unmagnetized bodies, in Introduction to Space Physics, ed. M. G. Kivelson and C. T. Russell (Cambridge University Press: Cambridge, UK), 203-225, 1995.

Lundin, R., S. Barabash, H. Andersson, *et al.*, Solar wind-induced atmospheric erosion at Mars: First results from ASPERA-3 on Mars Express, *Science*, **305**, 1933-1936, 2004.

Lundin, R., D. Winningham, S. Barabash, *et al.*, Ionospheric plasma acceleration at Mars: ASPERA-3 results, *Icarus*, **182**, 308-319, 2006.

Parks, G. K., Physics of Space Plasmas (Westview Press: Boulder, Colorado), 2004.

Vignes, D., C. Mazelle, H. Reme, et al., The solar wind interaction with Mars: Locations and shapes of the bow shock and the magnetic pile-up boundary from the observations of the MAG/ER Experiment onboard Mars Global Surveyor, *Geophys. Res. Lett.*, **27**, 49-52, 10.1029/1999GL010703, 2000.

Yamauchi, M., Y. Futaana, A. Fedorov, et al., IMF direction derived from cycloid-like ion distributions observed by Mars Express, *Space Sci. Rev.*, **126**, 239-266, 2006.

Yamauchi, M., Y. Futaana, A. Fedorov, et al., Comparison of accelerated ion populations observed upstream of the bow shocks at Venus and Mars, *Ann. Geophys.*, **29**, 511-528, 2011.

Yamauchi, M. R. Lundin, R. A. Frahm, et al., Oxygen foreshock of Mars, *Planet. Space Sci.*, **119**, 48-53, 2015.

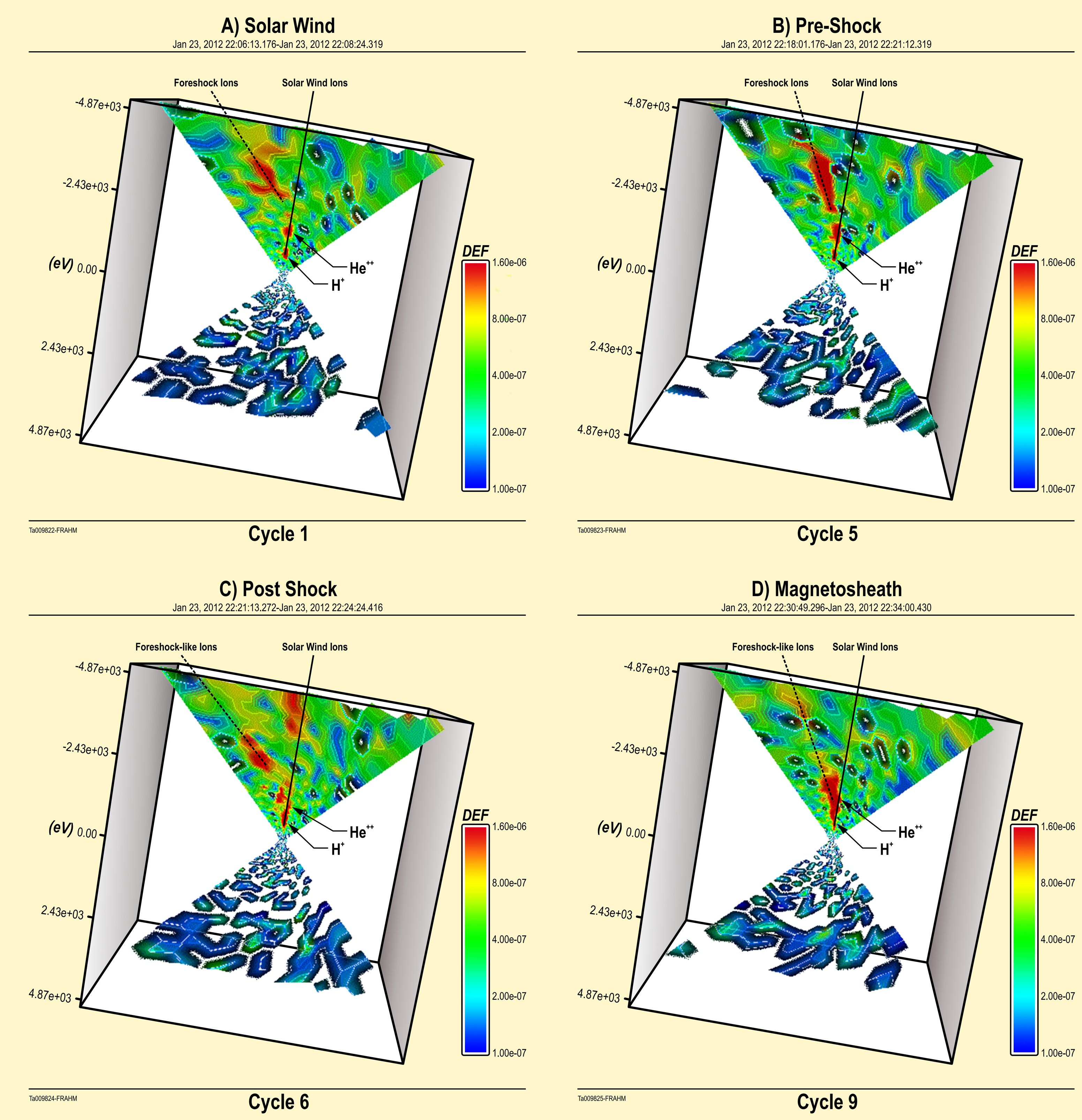

***Figure 6.** 3D Ion Distributions at Selected Instrument Cycles. The ion distribution in the solar wind (A), just before the bow shock (B), just inside the magnetosheath (C), and deep inside the magnetosheath (D) are generated in energy flux and show that the solar wind ion direction differs from that of foreshock and foreshock-like ions.*

Figure 6 shows four ion distributions which have been sliced to reveal the solar wind ions and the foreshock ions. The contours are generated by placing the energy flux value in a 3D energy-elevation angle-azimuthal angle array, contouring that volume, and then slicing that volume to show areas of ion flux intensification. Angular directions of foreshock and foreshock ions are indicated along with the direction of the solar wind H^+ and He^{++}. Panel A is from the solar wind where the foreshock ions are well developed. Panel B is just before the bow shock and the foreshock ions are separated from the solar wind ions. Panels C and D are from behind the bow shock, in the magnetosheath, and clearly show that the direction of the foreshock-like ions is not the same as the shocked solar wind.

Conclusion

Ions in the foreshock region of Mars were observed by the MEx particle detectors on 23 January 2012 between 2205 UT and 2221 UT. On this pass, the MEx spacecraft was moving inbound from the solar wind in the southern hemisphere from dawn, reaching periapsis on the dusk side of Mars near the equator at about 350 km altitude. The foreshock-like ions were observed to penetrate through multiple bow shock crossings and into the magnetosheath of Mars (to 2240 UT). Plasma measurements indicated that MEx crossed the bow shock three times while inbound from the solar wind (between 2221 UT and 2230 UT) with the solar wind reappearing just before the last bow shock crossing. The multiple bow shock crossing was most likely a transient feature based on additional passes through the same spatial region near the time of the measurements and multiple crossings over many years. Changes in the ion and electron pressure was not the likely cause of the bow shock location change, but magnetic pressure and IMF orientation cannot be ruled out as a possible cause.

Ions in the foreshock of the solar wind were observed to be beam-like around 20° from the solar wind direction. The ions had energies several times that of the solar wind protons. Foreshock-like ions were observed to penetrate into the magnetosheath and were observed until MEx was about a proton gyroradius from the bow shock. Shocked electron plasma indicated the presence of waves in the magnetosheath which could be reflecting a portion of the solar wind protons. It is expected that the frozen-in-flux assumption is violated within the bow shock region which would allow plasma to be generated at different angles to the magnetic field, allowing wave-particle reactions to generate the foreshock-like ion beams which are then transported into the foreshock region. The foreshock ions reflected from the bow shock are produced at a location upstream of the spacecraft while the spacecraft is in the solar wind. Foreshock-like ions could be locally produced deep inside the magnetosheath or at a location which is temporarily closer to the planet than the detected bow shock location.

It was observed that on this pass, ions in the magnetosheath could be separated into those within a proton gyroradius from the bow shock and those nearer the IMB. Those near the bow shock still retained their cold beam-like structure while those nearer the IMB were heated and flowed along the magnetosheath, in the direction of the tail of the magnetosphere.

Acknowledgements

The ASPERA-3 experiment on the European Space Agency (ESA) Mars Express mission is a joint effort between 15 laboratories in 10 countries, all sponsored by their national agencies. We thank all of these agencies as well as the various departments/institutions hosting these efforts. We wish to acknowledge support through the National Aeronautics and Space Administration (NASA) contract NASW-00003 in the United States, Science and Technology Facilities Council (STFC) in the United Kingdom, and the Swedish National Space Board for their support of the PI-Institute, the Swedish Institute of Space Physics (IRF). We thank C. A. Gonzalez, S. J. Jeffers, R. O. Menchaca, and M. A. Muller for technical assistance.